SCIENTIFIC REPORTS

OPEN

$TiO(OH)_2$ – highly effective catalysts for optimizing CO_2 desorption kinetics reducing CO_2 capture cost: A new pathway

Received: 9 February 2017
Accepted: 24 April 2017
Published online: 07 June 2017

Hongbao Yao[1,2], Sam Toan[1], Liang Huang[3], Maohong Fan[1,4], Yujun Wang[2], Armistead G. Russell[4], Guangsheng Luo[2] & Weiyang Fei[2]

The objective is to find a new pathway for significant reduction in CO_2 capture energy consumption. Specifically, nanoporous $TiO(OH)_2$ was used to realize the objective, which was desired as a catalyst to significantly accelerate the decomposition of aqueous $NaHCO_3$, essentially CO_2 desorption – the key step of $Na_2CO_3/NaHCO_3$ based CO_2 capture technologies from overall CO_2 energy consumption perspective. Effects of several important factors on $TiO(OH)_2$-catalyzed $NaHCO_3$ decomposition were investigated. The quantity of CO_2 generated from 0.238 mol/L $NaHCO_3$ at 65 °C with catalyst is ~800% of that generated without the presence of catalyst. When a 12 W vacuum pump was used for carrying the generated CO_2 out of reactor, the total amount of CO_2 released was improved by ~2,500% under the given experimental conditions. No significant decrease in the catalytic effect of $TiO(OH)_2$ was observed after five cyclic CO_2 activated tests. In addition, characterizations with *in-situ* Fourier transform infrared spectroscopy, thermal gravity analysis and Brunauer-Emmett-Teller of $TiO(OH)_2$ indicate that $TiO(OH)_2$ is quite stable. The discovery in this research could inspire scientists' interests in starting to focus on a new pathway instead of making huge effort or investment in designing high-capacity but expensive CO_2 sorbent for developing practical or cost-effective CO_2 technologies.

There is no doubt that countless progresses have been made in controlling SOx/NOx and Hg emissions from fossil fuel fired power plants[1]. However, the actions on CO_2 emission control have been slow[2]. The importance of CO_2 capture in fossil fuel-fired power plants cannot be underestimated any more due to the catastrophic effect of the continuous increase in CO_2 concentration in atmosphere and the ill effects it has on the environment[3–5], as indicated in the recently reached Paris Agreement[6].

Nowadays, chemical absorption by liquid solvents, including amines and carbonates, is widely considered to be the most promising method among various post-combustion CO_2 capture technologies[7–9]. However, high-energy requirements in the regeneration or CO_2 desorption process is the largest obstacle for preventing its industrial applications[10]. Conventional regenerations of spent solvents are just realized by heating spent solvents above boiling temperatures (100–150 °C). The energy consumption needed for CO_2 desorption or spent sorbent regeneration accounts for ~15–30% of power plants' electricity outputs[11].

Accordingly, many other efforts have been made for lowering CO_2 desorption energy consumptions and up to date, there mainly exists three important strategies[10–12]. The most popular one is to use new organic amine mixtures for CO_2 sorption and desorption. It was generally believed that adsorption solvents with lower heat of absorption require less heat to be regenerated. Thus, much attention has been focused on the blending of different types of amine solutions[12–14]. The other two strategies include the application of novel equipment with superior mass and heat transfer performance as well as process optimizations[12, 15]. For example, stripping CO_2 from aqueous potassium carbonate solutions was achieved by using two types of polymeric flat sheet microporous

[1]Department of Chemical and Petroleum Engineering, University of Wyoming, Laramie, WY, 82071, USA. [2]State Key Laboratory of Chemical Engineering, Department of Chemical Engineering, Tsinghua University, Beijing, 100084, China. [3]State Key Laboratory of Refractories and Metallurgy, Wuhan University of Science and Technology, Wuhan, 430081, China. [4]School of Civil and Environmental Engineering, Georgia Institute of Technology, Atlanta, Georgia, 30332, USA. Correspondence and requests for materials should be addressed to M.F. (email: mfan@uwyo.edu) or Y.W. (email: wangyujun@mail.tsinghua.edu.cn)

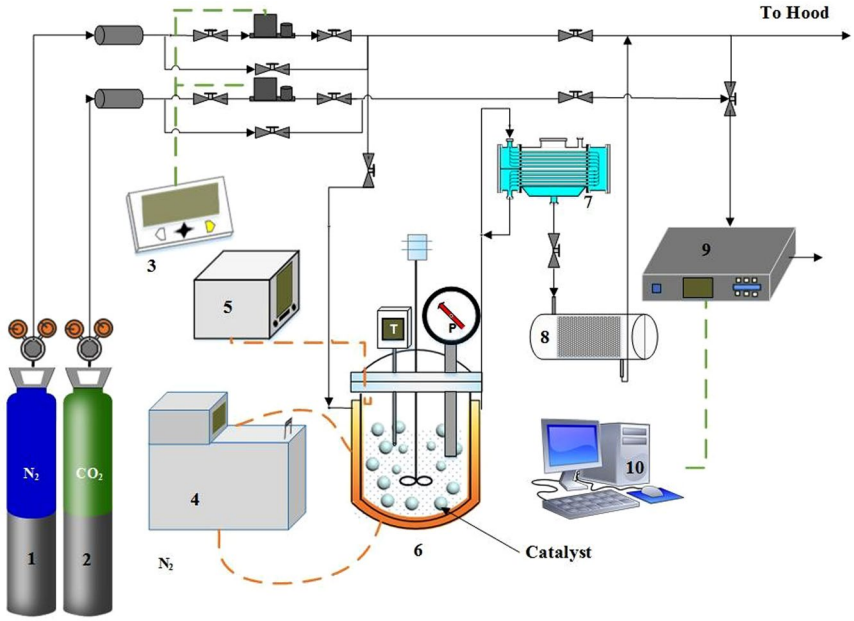

Figure 1. Schematic diagram of CO_2 desorption set-up [1: N_2 cylinder; 2: CO_2 cylinder; 3: mass flow controller; 4: thermostatic water bath; 5: thermoelectric couple; 6: stirred tank reactor; 7; condenser; 8: desiccator; 9; gas concentration analyzer; 10: data recording unit].

membrane contactors, which have been reported by Michael and co-workers[16]. Unfortunately, the efforts made in promoting CO_2 desorption or spent sorbent regeneration are still much less than that improving CO_2 absorption.

On the other hand, it should be pointed out that amine solvents, such as monoethanolamine (MEA), diethanolamine (DEA) and methyldiethanolamine (MDEA), have several serious shortcomings such as toxicity, corrosiveness, and oxidative degradation[17, 18]. Alternative sorbents are inorganic carbonate solutions based on Equation R1, in which M stands for Na or K.

$$M_2CO_3 + CO_2 + H_2O \leftrightarrow 2MHCO_3. \quad \text{R1}$$

R1 based CO_2 captures are not only inexpensive but also stable and thus environmentally friendly. However, like any other CO_2 sorbents, its slow CO_2 desorption kinetics make its wide utilization unaffordable, considering the fact that the energy consumption of the CO_2 desorption step accounts for ~70–80% of those needed for the corresponding overall CO_2 capture processes[19].

This research was designed to fill the gap with its focus on investigating the significant effect of $TiO(OH)_2$ on promoting aqueous $NaHCO_3$ decomposition or CO_2 desorption kinetics and the cost of $Na_2CO_3/NaHCO_3$ based CO_2 capture technology. The success could lead to a new pathway for future CO_2 capture technology development with its focus on catalysis instead of high-capacity but expensive sorbents.

Results

Effects of several key factors on the performance of $TiO(OH)_2$ on $NaHCO_3$ decomposition, essentially CO_2 desorption. *Stirring rate.* The experimental set-up for aqueous $NaHCO_3$ decomposition or CO_2 desorption test is illustrated in Fig. 1. The photo of actual experimental set-up is provided in supporting information (SI Photo 1). The quantities of CO_2 desorbed under different stirring rates at the given temperature (70 °C) were first evaluated. As shown in Fig. 2, CO_2 desorption amounts increase with the increase in stirring rates ranging from 400 rpm to 550 rpm while stirring rate only shows slight effect when it increases from 600 rpm to 650 rpm. This means that the mass transfer resistance of CO_2 diffusing from liquid phase to gas phase was intensively reduced and thus, CO_2 desorption is dominated by its reaction kinetics when stirring rate is higher than 600 rpm under experimental conditions.

Quantity of $TiO(OH)_2$ added. The effect of the quantity of $TiO(OH)_2$ or the Ti/Na molar ratio in solution on the decomposition of $NaHCO_3$ is shown in Fig. 3. $NaHCO_3$ decomposition or CO_2 desorption significantly increases with the quantity of added $TiO(OH)_2$ or the Ti/Na ratio. However, the improvement sensitivity decreases with Ti/Na ratio. Under the test conditions, the highest improvement in $NaHCO_3$ decomposition or CO_2 desorption reaches 800% at 110 s of reaction time. Considering the fact that the quantity of H_2O in reactor is much more than that stoichiometrically needed, the promotional effect of $TiO(OH)_2$ on $NaHCO_3$ decomposition or CO_2 desorption is exceptional.

Temperature. The effects of $TiO(OH)_2$ on $NaHCO_3$ decomposition or CO_2 desorption kinetics at temperatures of 40 °C, 50 °C, 60 °C and 70 °C are presented in Fig. 4. The quantity of CO_2 released within the first 180 seconds with the use of $TiO(OH)_2$ at 40 °C is 2.79 mmol, ~510% higher than that obtained without use of $TiO(OH)_2$ under

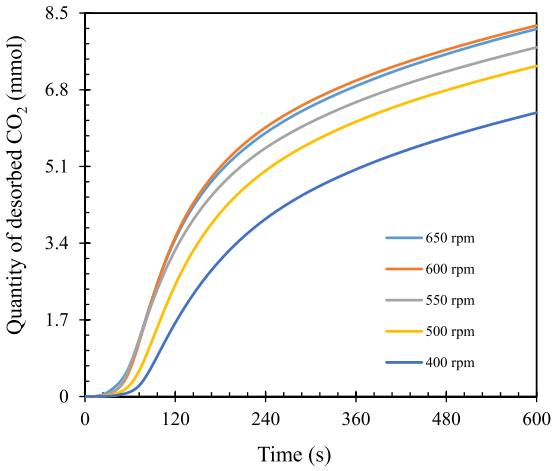

Figure 2. $NaHCO_3$ decomposition or CO_2 desorption profiles under different stirring rates [initial $NaHCO_3$ concentration: 0.143 mol/L; Ti/Na molar ratio: 0.78; reaction temperature: 70 °C; N_2 flow rate: 500 mL/min].

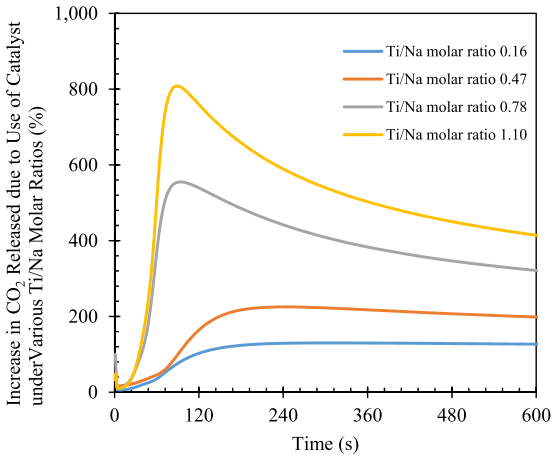

Figure 3. Effect of Ti/Na molar ratio on $NaHCO_3$ decomposition or CO_2 desorption [initial $NaHCO_3$ concentration: 0.238 mol/L; stirring rate: 600 rpm; reaction temperature: 65 °C; N_2 flow rate: 500 mL/min].

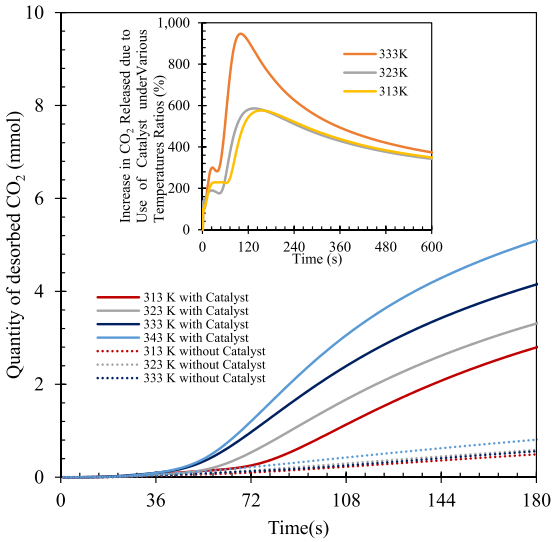

Figure 4. Effect of temperature on catalytic $NaHCO_3$ decomposition or CO_2 desorption [initial $NaHCO_3$ concentration: 0.143 mol/L; Ti/Na molar ratio: 0.78; stirring rate: 600 rpm; N_2 flow rate: 500 mL/min].

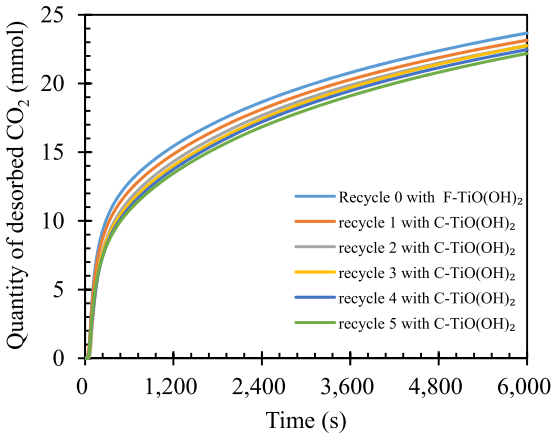

Figure 5. Cyclic performance of $TiO(OH)_2$ on $NaHCO_3$ decomposition [initial $NaHCO_3$ concentration: 0.238 mol/L; Ti/Na molar ratio: 0.78, stirring rate: 600 rpm; reaction temperature: 60 °C, N_2 flow rate: 500 mL/min].

	Specific surface area (m^2/g)	Pore volume (cm^3/g)	Pore diameter (Å)
F-$TiO(OH)_2$	807.4	0.73	17.12
C-$TiO(OH)_2$ after 5 cycles	693.1	0.66	17.08

Table 1. BET characteristics of F-$TiO(OH)_2$ and C-$TiO(OH)_2$.

the same condition. At 70 °C, the catalyst can improve $NaHCO_3$ decomposition by about 490% within the first 180 s. The catalytic effects gradually decrease with time as dictated with thermodynamic theories, although they are still considerably large after 600 s of $NaHCO_3$ decomposition. For example, 5.63 mmol of CO_2 was released with the use of $TiO(OH)_2$ at 40 °C after 600 s, while only 1.61 mmol of CO_2 was released without presence of $TiO(OH)_2$under the same conditions, a 71.4% decrease.

Cyclic performance of $TiO(OH)_2$ on $NaHCO_3$ decomposition. In addition, the regeneration performance of $NaHCO_3$ solution decomposition using $TiO(OH)_2$ plays a key role in practical applications and cannot be neglected, which has also been examined in detail in this work. The fresh $TiO(OH)_2$ and CO_2-treated $TiO(OH)_2$ or cycled $TiO(OH)_2$ are hereafter denoted as F-$TiO(OH)_2$ and C-$TiO(OH)_2$, respectively. The C-$TiO(OH)_2$ promoted CO_2 release curves obtained from aqueous $NaHCO_3$ are almost overlap and no remarkable decrease in the total CO_2 desorption amounts are noticed in five continuous cycles as shown in Fig. 5. Furthermore, considering the resulting pore structure data summarized in Table 1, the specific surface area and pore volume of C-$TiO(OH)_2$ after 5 cycles of uses are 693.1 m^2/g and 0.658 cm^3/g, respectively, are comparable to those of F-$TiO(OH)_2$. This suggests that $TiO(OH)_2$ is a stable catalyst for $NaHCO_3$ decomposition or CO_2 desorption.

Discussion

N_2 adsorption/desorption isotherms and pore-size distributions were conducted to investigate the pore structures of F-$TiO(OH)_2$ and C-$TiO(OH)_2$ with 5 cycles of CO_2 desorption and sorption. The resulting pore structure data were summarized in Table 1. Both samples are nanoporous with the average diameter close to 1.7 nm. The specific surface area of F-$TiO(OH)_2$ could reach to as high as 807.4 m^2/g, while that of C-$TiO(OH)_2$ is 693.1 m^2/g, about a 14% drop.

The FT-IR absorption spectra of two $TiO(OH)_2$ samples, Na_2CO_3 and $NaHCO_3$ are shown in Fig. 6. Both $TiO(OH)_2$ samples show broad peaks in the 400–900 cm^{-1} range corresponding to Ti-O bending. The additional peaks in the 3,000–3,600 cm^{-1} range existing in C-$TiO(OH)_2$ sample are likely due to the partial hydration during the reaction process. Typically, two small peaks at 1,124 and 1,072 cm^{-1} in the F-$TiO(OH)_2$ likely result from Ti-O-C, the ending and bridging isopropyl groups, considering that $TiO(OH)_2$ are directly synthesized from the hydrolysis of TTIP. Similar phenomena were also reported by Sui and coworkers[20]. Small peaks at 1,132, 1,117 and 1,022 cm^{-1} were associated with Ti-O-C and butoxyl groups. In addition, it should be noted that C-O-H bending vibrations could appear as a broad and weak peak at 1,440–1,220 cm^{-1} in alcohols and phenols[21,22]. Accordingly, the two small peaks observed at 1,124, 1,072 cm^{-1} for F-$TiO(OH)_2$ and C-$TiO(OH)_2$ may also be related to Ti-O-H group, which may be the major player in accelerating $NaHCO_3$ decomposition or CO_2 desorption.

Moreover, the FT-IR spectra of the $NaCO_3$ and $NaHCO_3$ obtained in experiments are consistent with those in references[23–25]. The noteworthy peaks at 1,300 cm^{-1} and 1,400 cm^{-1} for $NaHCO_3$ and Na_2CO_3, respectively, are due to carbonate asymmetric stretching[26]. In addition, a peak at 1,605 cm^{-1} was observed for $NaHCO_3$, which

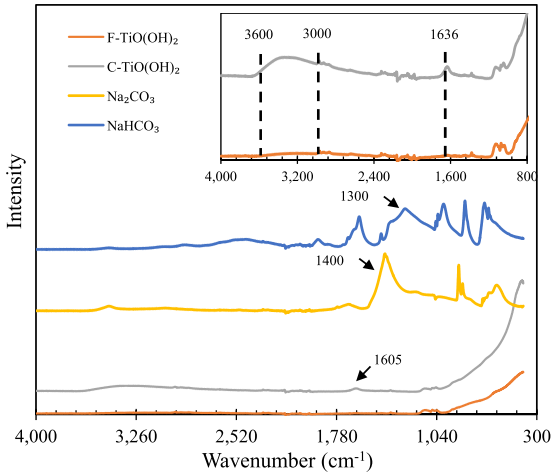

Figure 6. FT-IR spectra of F-$TiO(OH)_2$, C-$TiO(OH)_2$, Na_2CO_3, and $NaHCO_3$.

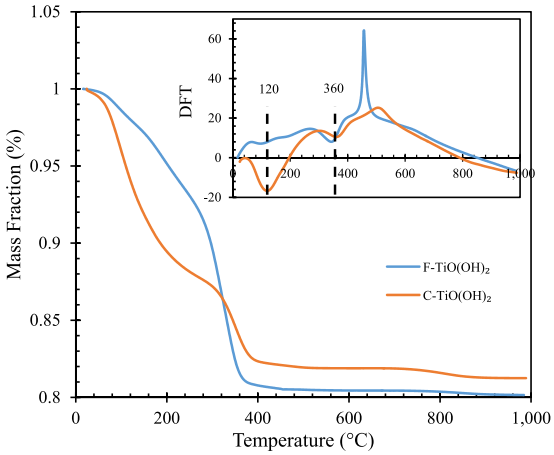

Figure 7. TGA data of F-$TiO(OH)_2$ and C-$TiO(OH)_2$ [heating rate: 20 °C/min; N_2 flow rate: 100 mL/min].

can be attributed to symmetric stretching of CO_2. Therefore, the peak at 1,636 cm^{-1} for C-$TiO(OH)_2$ may be due to the presence of CO_3^{2-} or HCO_3^-. This indicates that $NaHCO_3$ or $NaCO_3$ may be sorbed on the inner pore of F-$TiO(OH)_2$, which could be responsible for the decrease in specific surface area of C-$TiO(OH)_2$ as observed in Table 1.

The TGA data of F-$TiO(OH)_2$ and C-$TiO(OH)_2$ are shown in Fig. 7. Both samples started to lose absorbed water at ~120 °C, and then decomposed to TiO_2 above 300 °C. The final masses of F-$TiO(OH)_2$ and C-$TiO(OH)_2$ account for 80.1% and 81.2% of their initial masses, respectively, indicating that no titanium loss took place during the $NaHCO_3$ decomposition or CO_2 desorption process in this research. F-$TiO(OH)_2$ shows slower mass loss rates at lower temperatures, which could be due to loss of organic groups[27] from TTIP. This agrees with what was observed in the FTIR results.

Furthermore, Raman spectroscopy analyses of F-$TiO(OH)_2$, C-$TiO(OH)_2$, pure Na_2CO_3 and $NaHCO_3$ were also conducted and the results are shown in Fig. 8. All samples have a similar broad band in the range of 3,000–3,200 cm^{-1}, which resulted from H-O vibration in the water absorbed from air[28]. Two very strong peaks at *ca* 1,043 cm^{-1} for $NaHCO_3$ and at *ca* 1,079 cm^{-1} for Na_2CO_3 were observed, which has been reported by others[29,30] and can both be assigned to the ν_1 symmetric stretch.

Both $TiO(OH)_2$ samples show relatively intense Raman bands at *ca* 446 cm^{-1} and *ca* 636 cm^{-1} (*ca* 584 cm^{-1} for reacted $TiO(OH)_2$). Typically, the frequencies of the Raman bands observed are 513 cm^{-1} and 636 cm^{-1} for anatase and 446 cm^{-1} and 609 cm^{-1} for rutile, respectively[29,31,32]. The $TiO(OH)_2$ sample in this work is amorphous and the position and intensity of its characteristic peaks can be changed by modifying its material structures. It should be pointed out that the resulting Raman spectrum for C-$TiO(OH)_2$ is quite similar to that of F-$TiO(OH)_2$, implying that $TiO(OH)_2$ is stable or can be cyclically used.

Finding a cost-effective method for carrying the released or desorbed CO_2 out of reaction system is important. A pump was used to compare its performance on carrying the released CO_2 out of its desorption system to that achieved with N_2 as a carrier gas, and the results obtained within 55–65 °C are shown in Fig. 9. It can be seen that the quantity of CO_2 carried out with N_2 was high than that with a pump when $NaHCO_3$ decomposition was not

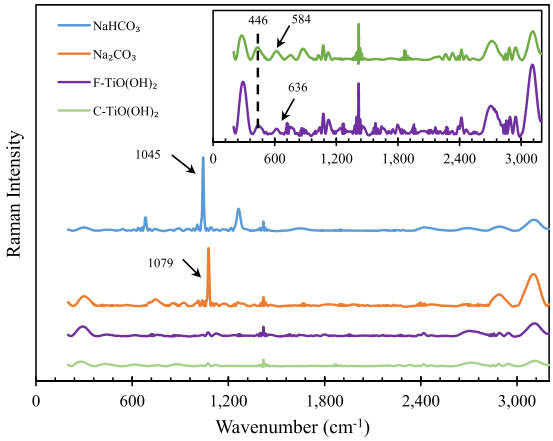

Figure 8. Raman spectra of F-$TiO(OH)_2$, C-$TiO(OH)_2$, pure Na_2CO_3 and $NaHCO_3$.

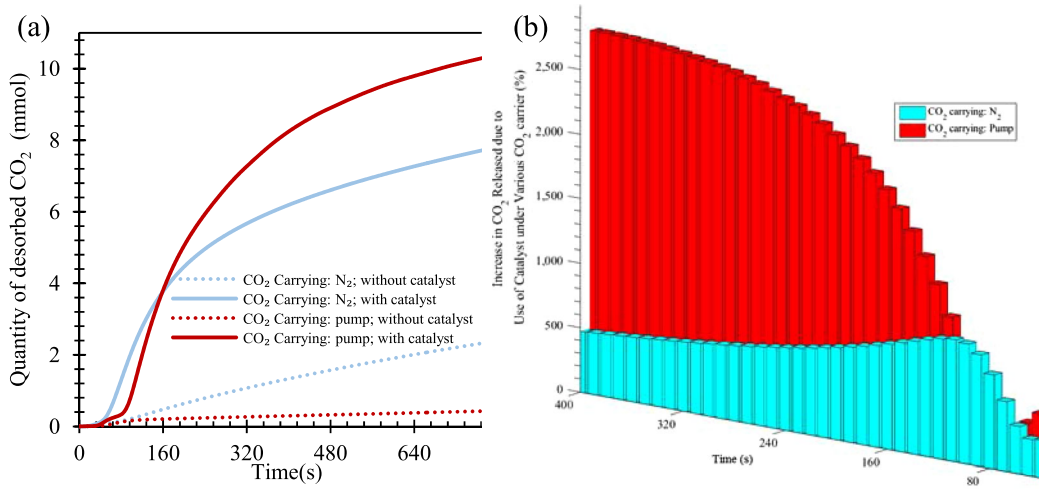

Figure 9. (**a**) Effect of different CO_2 carrying out methods on CO_2 release [initial $NaHCO_3$ concentration: 0.238 mol/L; Ti/Na molar ratio: 0.78; stirring rate: 600 rpm; reaction temperature: 65 °C, N_2 flow rate: 200 mL/min; power of pump: 12 W]. (**b**) Ratio of CO_2 released by using N_2 gas and the pump with and without uses of catalyst for each 10 seconds.

catalyzed with $TiO(OH)_2$. However, the pump carried out 25% more CO_2 than the same amount of N_2 did when the catalyst was used. The quantity of the CO_2 generated from non-catalytic $NaHCO_3$ decomposition with 200 ml/min N_2 being a carrier gas is only ~1/8 of that from catalytic $NaHCO_3$. Furthermore, when a 12 W pump was used for carrying the generated CO_2 out of $NaHCO_3$ decomposition reactor, the CO_2 releasing improvement due to the help of the catalyst is about 25 times or 2,500%.

Figures 3, 4 and 9 clearly show that noticeable CO_2 release from catalytic $NaHCO_3$ decomposition was observed earlier than that from non-catalytic $NaHCO_3$ decomposition. This is not only confirmed with the experimental set-up shown in Fig. 1 but also with the data collected with the FTIR function of the available *in-situ* FTIR-MS (SI Photo 2) for solid $NaHCO_3$ decomposition and shown in Fig. 10. The time needed for the appearing of the peak of C=O in the released CO_2 of catalytic $NaHCO_3$ decomposition is longer than that of non-catalytic $NaHCO_3$ decomposition.

Conclusion

Nanoporous $TiO(OH)_2$ is a very effective catalyst for aqueous $NaHCO_3$ decomposition or CO_2 desorption, and thus CO_2 capture. The finding could be significantly helpful for reducing the global concern about the high energy consumption required for CO_2 emission control. Further works should focus on understanding the associated mechanism and extending the new concept to other CO_2 emission and utilization technologies development.

Methods

$TiO(OH)_2$ preparation. Titanium isopropoxide (TTIP), ethanol (EtOH) and sodium bicarbonate ($NaHCO_3$) were purchased from Sigma-Aldrich and used without any further purification prior to preparing $TiO(OH)_2$. The first $TiO(OH)_2$ preparation step was to add 25 mL titanium isopropoxide to 350 mL deionized water at room

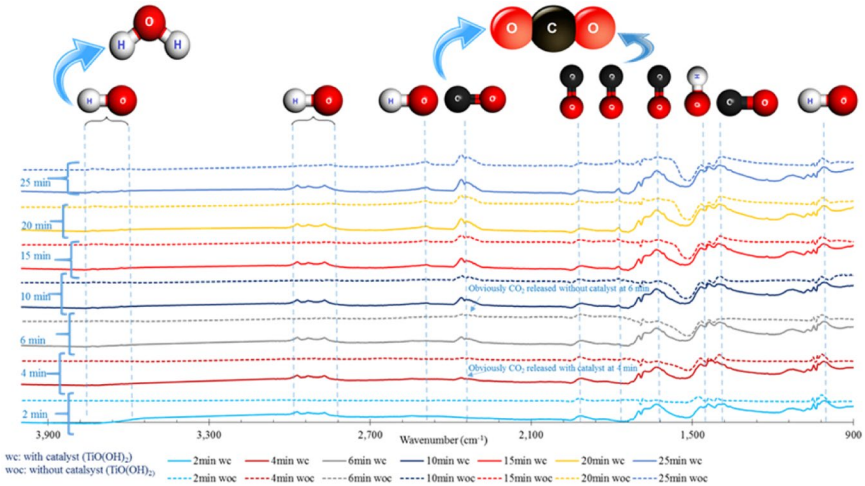

Figure 10. FT-IR- characterization of catalytic and non-catalytic solid $NaHCO_3$ decomposition [$NaHCO_3$: $TiO(OH)_2$ mole ratio: 1:2; temperature: 150 °C; He flow rate: 5 ml/min].

temperature, followed by 4 hours of vigorous stirring. The resulting white precipitate was separated by filtration, and then washed several times with deionized water and anhydrous ethanol sequentially. The wet $TiO(OH)_2$ was dried under 120 °C in an oven for 12 h.

$TiO(OH)_2$ characterization. The Brunauer-Emmett-Teller (BET) surface areas and pore size distribution of $TiO(OH)_2$ samples were measured by using a Quantachrome Autosorb-iQ pore structure analyzer. Pore volumes were estimated from the adsorbed amount of N_2 at a relative pressure of $P/P_0 = 0.99$. Fourier transformed-infrared (FTIR) spectroscopy data were collected with a Thermo Nicolet Magna-IR 760 spectrometer (SI Photo 1). Thermal gravity analysis (TGA) tests were conducted on a TA Instruments SDT Q600 thermogravimetric analyzer. Raman spectra of the $TiO(OH)_2$ samples were collected on a Raman Sierra IM-52 instrument from Snowy Range Instruments with a 532 nm laser and 3 mW power.

$NaHCO_3$ decomposition or CO_2 desorption tests. $NaHCO_3$ decomposition tests were started by adding predetermined amounts of $TiO(OH)_2$, $NaHCO_3$ and deionized water into the reactor stirred at the rate of 600 rpm. Reaction temperatures were regulated using a digital temperature controller. During $NaHCO_3$ decomposition, pure N_2 or vacuum pump (Karlsson Robotics, 12 W) was used to carry the desorbed CO_2 out of reactor. The change of CO_2 outlet concentration with time was recorded in a data acquisition unit, and the concentration-time profile was used to calculate the quantity of CO_2 desorbed and evaluated to observe the difference in CO_2 desorption due to the use of $TiO(OH)_2$. When $TiO(OH)_2$ was used for cyclic $NaHCO_3$ decomposition or CO_2 desorption tests, the used $TiO(OH)_2$ and deionized water were mixed in a closed tank with pure CO_2 at 200 psi followed by vigorous stirring under room temperature to study the effect of CO_2 sorption or activation on $TiO(OH)_2$.

References

1. Ling, L. X., Fan, M. H., Wang, B. J. & Zhang, R. G. Application of computational chemistry in understanding the mechanisms of mercury removal technologies: a review. *Energy & Environmental Science* **8**, 3109–3133, doi:10.1039/c5ee02255j (2015).
2. Cui, S. *et al.* Mesoporous amine-modified SiO_2 aerogel: a potential CO_2 sorbent. *Energy & Environmental Science* **4**, 2070–2074, doi:10.1039/c0ee00442a (2011).
3. Boot-Handford, M. E. *et al.* Carbon capture and storage update. *Energy & Environmental Science* **7**, 130–189, doi:10.1039/c3ee42350f (2014).
4. Zhang, Z., Yao, Z.-Z., Xiang, S. & Chen, B. Perspective of microporous metal-organic frameworks for CO_2 capture and separation. *Energy & Environmental Science* **7**, 2868–2899, doi:10.1039/c4ee00143e (2014).
5. Kong, Y. *et al.* A new aerogel based CO_2 adsorbent developed using a simple sol-gel method along with supercritical drying. *Chemical Communications* **50**, 12158–12161, doi:10.1039/c4cc06424k (2014).
6. *Paris Agreement*, 2016. https://treaties.un.org/pages/ViewDetails.aspx?src=TREATY&mtdsg_no=XXVII-7d&chapter=27&clang=_en.
7. Dutcher, B., Fan, M. & Russell, A. G. Amine-Based CO_2 Capture Technology Development from the Beginning of 2013-A Review. *Acs Applied Materials & Interfaces* **7**, 2137–2148, doi:10.1021/am507465f (2015).
8. Liang, Z. *et al.* Recent progress and new developments in post-combustion carbon-capture technology with amine based solvents. *International Journal of Greenhouse Gas Control* **40**, 26–54, doi:10.1016/j.ijggc.2015.06.017 (2015).
9. Sharma, S. D. & Azzi, M. A critical review of existing strategies for emission control in the monoethanolamine-based carbon capture process and some recommendations for improved strategies. *Fuel* **121**, 178–188, doi:10.1016/j.fuel.2013.12.023 (2014).
10. Li, T. & Keener, T. C. review: Desorption of CO_2 from rich solutions in chemical absorption processes. *International Journal of Greenhouse Gas Control* **51**, 290–304, doi:10.1016/j.ijggc.2016.06.030 (2016).
11. Singh, P. & Versteeg, G. F. Structure and activity relationships for CO_2 regeneration from aqueous amine-based absorbents. *Process Safety and Environmental Protection* **86**, 347–359, doi:10.1016/j.psep.2008.03.005 (2008).
12. Zhang, X. *et al.* Experimental studies of regeneration heat duty for CO_2 desorption from diethylenetriamine (DETA) solution in a stripper column packed with Dixon ring random packing. *Fuel* **136**, 261–267, doi:10.1016/j.fuel.2014.07.057 (2014).

13. Oexmann, J. & Kather, A. Minimising the regeneration heat duty of post-combustion CO_2 capture by wet chemical absorption: The misguided focus on low heat of absorption solvents. *International Journal of Greenhouse Gas Control* **4**, 36–43, doi:10.1016/j.ijggc.2009.09.010 (2010).
14. Sakwattanapong, R., Aroonwilas, A. & Veawab, A. Behavior of reboiler heat duty for CO_2 capture plants using regenerable single and blended alkanolamines. *Industrial & Engineering Chemistry Research* **44**, 4465–4473, doi:10.1021/ie050063w (2005).
15. Frimpong, R. A., Remias, J. E., Neathery, J. K. & Liu, K. Solvent regeneration with a high volatility liquid as stripping carrier. *International Journal of Greenhouse Gas Control* **9**, 124–129, doi:10.1016/j.ijggc.2012.03.014 (2012).
16. Simioni, M., Kentish, S. E. & Stevens, G. W. Membrane stripping: Desorption of carbon dioxide from alkali solvents. *Journal of Membrane Science* **378**, 18–27, doi:10.1016/j.memsci.2010.12.046 (2011).
17. Knuutila, H., Juliussen, O. & Svendsen, H. F. Kinetics of the reaction of carbon dioxide with aqueous sodium and potassium carbonate solutions. *Chemical Engineering Science* **65**, 6077–6088, doi:10.1016/j.ces.2010.07.018 (2010).
18. Savage, D., Sartori, G. & Astarita, G. Amines as rate promoters for carbon dioxide hydrolysis. *Faraday Discussions of the Chemical Society* **77**, 17–31, doi:10.1039/dc9847700017 (1984).
19. Feng, B., Du, M., Dennis, T. J., Anthony, K. & Perumal, M. J. Reduction of Energy Requirement of CO_2 Desorption by Adding Acid into CO_2-Loaded Solvent. *Energy & Fuels* **24**, 213–219, doi:10.1021/ef900564x (2010).
20. Sui, R., Rizkalla, A. S. & Charpentier, P. A. FTIR study on the formation of TiO_2 nanostructures in supercritical CO_2. *The Journal of Physical Chemistry B* **110**, 16212–16218, doi:10.1021/jp0570521 (2006).
21. Colthup, N. *Introduction to infrared and Raman spectroscopy*. (Elsevier, 2012).
22. Schrader, B. *Infrared and Raman spectroscopy: methods and applications*. (John Wiley & Sons, 2008).
23. Nickolov, Z. S., Ozcan, O. & Miller, J. FTIR analysis of water structure and its significance in the flotation of sodium carbonate and sodium bicarbonate salts. *Colloids and Surfaces A: Physicochemical and Engineering Aspects* **224**, 231–239, doi:10.1016/S0927-7757(03)00317-0 (2003).
24. Dutcher, B., Fan, M. & Leonard, B. Use of multifunctional nanoporous $TiO(OH)_2$ for catalytic $NaHCO_3$ decomposition-eventually for $Na_2CO_3/NaHCO_3$ based CO_2 separation technology. *Separation and Purification Technology* **80**, 364–374, doi:10.1016/j.seppur.2011.05.022 (2011).
25. Dutcher, B. *et al*. Use of Nanoporous FeOOH as a Catalytic Support for $NaHCO_3$ Decomposition Aimed at Reduction of Energy Requirement of $Na_2CO_3/NaHCO_3$ Based CO_2 Separation Technology. *Journal of Physical Chemistry C* **115**, 15532–15544, doi:10.1021/jp204899r (2011).
26. Su, C. M. & Suarez, D. L. *In situ* infrared speciation of absorbed carbonate on aluminum and iron oxide. *Clays and Clay Minerals* **45**, 814–825, doi:10.1346/ccmn.1997.0450605 (1997).
27. Sui, R. H., Rizkalla, A. S. & Charpentier, P. A. FTIR study on the formation of TiO_2 nanostructures in supercritical CO_2. *Journal of Physical Chemistry B* **110**, 16212–16218, doi:10.1021/jp0570521 (2006).
28. Wu, J. & Zheng, H. Quantitative measurement of the concentration of sodium carbonate in the system of Na_2CO_3-H_2O by Raman spectroscopy. *Chemical Geology* **273**, 267–271, doi:10.1016/j.chemgeo.2010.03.001 (2010).
29. de Veij, M., Vandenabeele, P., De Beer, T., Remonc, J. P. & Moens, L. Reference database of Raman spectra of pharmaceutical excipients. *Journal of Raman Spectroscopy* **40**, 297–307, doi:10.1002/jrs.2125 (2009).
30. Brooker, M. & Bates, J. B. Raman and infrared spectral studies of anhydrous Li_2CO_3 and Na_2CO_3. *The Journal of Chemical Physics* **54**, 4788–4796, doi:10.1063/1.1674754 (1971).
31. Balachandran, U. & Eror, N. G. Raman spectra of titanium dioxide. *Journal of Solid State Chemistry* **42**, 276–282, doi:10.1016/0022-4596(82)90006-8 (1982).
32. Rigby, S. J., Al-Obaidi, A. H. R., Lee, S.-K., McStay, D. & Robertson, P. K. J. The application of Raman and anti-stokes Raman spectroscopy for *in situ* monitoring of structural changes in laser irradiated titanium dioxide materials. *Applied Surface Science* **252**, 7948–7952, doi:10.1016/j.apsusc.2005.10.003 (2006).

Acknowledgements
The authors gratefully acknowledge the great support from the Department of Energy, State of Wyoming.

Author Contributions
Hongbao Yao, Sam Toan and Liang Huang performed the experiments. Hongbao Yao analyzed data and wrote the whole manuscript. Sam Toan helped to draw Figures 9 and 10. Liang Huang helped to draw the graphic abstract. Maohong Fan and Yujun Wang supervised the study, planned and designed experiments. Armistead G. Russell, Guangsheng Luo and Weiyang Fei helped in editing the manuscript. All authors reviewed the manuscript.

Additional Information
Supplementary information accompanies this paper at doi:10.1038/s41598-017-03125-w

Competing Interests: The authors declare that they have no competing interests.

Publisher's note: Springer Nature remains neutral with regard to jurisdictional claims in published maps and institutional affiliations.